Forces and structure in thin liquid soap films

1999 J. Phys.: Condens. Matter 11 R215

(http://iopscience.iop.org/0953-8984/11/19/201)

J. Phys.: Condens. Matter **11** (1999) R215–R238. Printed in the UK PII: S0953-8984(99)83711-4

REVIEW ARTICLE

Forces and structure in thin liquid soap films

Vance Bergeron

Rhône Poulenc Industrialisation, 85, Avenue Des Freres Perret, BP 62, Saint-Fons Cédex, France

Received 11 January 1999

Abstract. This review is a topical survey of the forces and structures in thin liquid soap films. Included is a description of both the more classical forces, such as electrostatic double-layer and dispersion forces, together with new and emerging areas of research that cover so-called 'supramolecular' forces. This latter category covers self-assembly of macromolecular structures confined in a thin-film region together with surface-induced adsorption of macromolecular complexes. In addition, recent extensions of the relation between thin-film forces and film stability are reviewed.

Contents

1. Introduction

Over the centuries thin liquid soap films have been both the subject of fascination and discovery throughout physics. As early as the late 17th century some of the first recorded observations using soap films were reported by Hooke and Newton during their efforts to understand the reflections, refractions and colours of light; work which laid the groundwork for the modern theory of light [1, 2]. Likewise, the great accomplishments of Plateau in the nineteenth century, concerning minimal surfaces and their forms, also relied on rigorous observations of soap films. Continuing the list of prodigious works into the present century leads to Gibbs' and Maringoni's thermodynamic descriptions of thin films, and the collected works

of Derjaguin and Overbeek, which culminated in the celebrated DLVO theory (named after its founders, Derjaguin, Landau, Verwey and Overbeek) that accounts for the basic molecular forces operative within thin liquid films [3, 4]. This later work serves as the foundation for describing colloid stability and its essentials and advances over the last few decades are the focus of the present review.

In particular, the colloidal systems addressed here are foams (gas liquid dispersions) and emulsions (liquid–liquid dispersions). As these systems are composed of one phase dispersed within another it is important to realize that the overall stability of these systems relies on the stability of the individual films of intervening continuous phase that separate the discontinuous phases (e.g. soap films) (figure 1). Hence detailed knowledge of the formation and stability of these intervening films permits rational utilization of foam and emulsion systems for a broad range of applications. Thus, a great deal of effort has been spent studying the dynamics and stability of individual thin liquid films [5, 6].

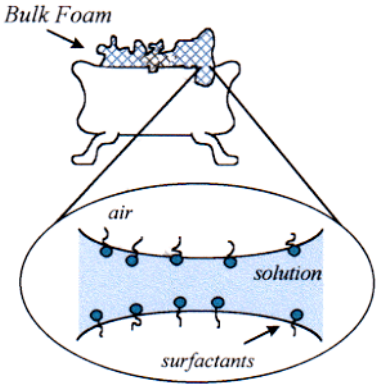

Figure 1. Foam is a dispersion of gas in a liquid solution which forms a collection of thin liquid films. The stability of these films is governed by surface active molecules ('surfactants') that adsorb to the solution–air interface.

Equally important to recognize is the fact that foams and emulsions are in an absolute sense thermodynamically unstable; however, it is often found that a particular system can be categorized as a relatively short-lived 'dynamically' stabilized system (∼minutes) or one that can remain stable for very long periods (∼days or years). Champagne foams are a classic example of the former, while robust beer foams and cosmetic creams fall into the latter category. This striking difference in a dispersion's lifetime reflects the primary mechanisms that govern the stability of the individual films comprising its structure. In rapidly coalescing dispersions, the film lifetimes are controlled by the drainage rate of the intervening continuous phase (i.e. hydrodynamic phenomena), while the long-lived systems require additional time to overcome energy barriers that hold the film in a metastable thermodynamic state, see figure 2. These barriers arise from surface-force interactions (i.e. disjoining pressures) created by having two interfaces in close proximity. In fact, for some cases overcoming these barriers can take so long that other factors such as Ostwald ripening and gas diffusion determine the ultimate lifetime of the dispersion. Clearly, understanding and controlling the energy barriers that inhibit thin-film coalescence has great practical benefits for the utilization of these dispersed systems. To this end, the central theme of this work is to present the various intermolecular forces and structures that arise in surfactant-laden thin-liquid films and to show how they are quantified and studied experimentally.

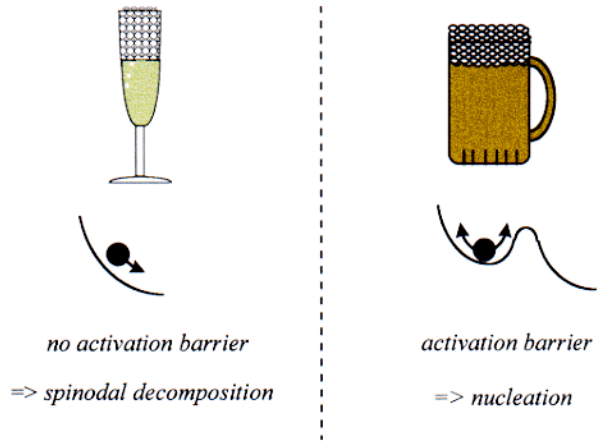

Figure 2. Typically foams can be categorized as short-lived systems where film rupture is described as a spinodal decomposition (champagne foams), or long-lived systems in which energy barriers create an activation energy and film rupture is governed by a nucleation process (robust beer foams).

2. Disjoining pressure (surface forces)

The *disjoining pressure* is a concept traditionally used in the field of foams and emulsions (fluid systems) which is completely analogous to what is commonly referred to as *surface forces* when considering interactions in thin films that separate two solid phases (e.g. solid dispersions). The primary difference is simply based on the historical origins of the different schools working on the subject. As the present work is focused on fluid systems, we adopt the former to be historically consistent.

2.1. Mechanical definition

Every interface has a thin interfacial transition region whose intensive thermodynamic properties deviate from those of the two neighbouring bulk phases. These transition regions naturally develop from changes in the molecular interactions as we cross a phase boundary. If two interfaces approach one another these molecular interactions manifest themselves as macroscopic forces of interaction between the interfaces. This situation will occur when any two phases approach each other while an intervening third phase separating them grows thinner (e.g. foam film—separation of two gas phases by an intervening solution). When the thickness of the intervening phase becomes comparable to the thickness of the interfacial regions there remains no portion of the interlayer (i.e. film) possessing the properties of the initial intervening 'bulk' phase and further decreases in film thickness require work. This requirement originates from net repulsive or attractive macroscopic forces generated by the overlapping interfacial regions. Therefore, in order to maintain a constant film thickness after interfacial overlapping has occurred, an external force (positive or negative) must be applied to the system. A crude but simple analogy to this process is found by considering what happens when two magnets are brought together. As the magnets approach and their fields start to overlap, an additional external pressure must be applied in order to bring them closer (this can be a negative or positive pressure depending on the interaction between the magnets). Similarly, as the intervening aqueous solution in a thin liquid film (e.g. foam, emulsion etc) drains, the interfaces approach one another and the phases separated by the solution interact. These interactions can be

quantified as an excess pressure versus the separation distance (i.e. the film thickness, h), which by definition is a *disjoining pressure isotherm*. Note that the term disjoining is somewhat misleading in that attractive forces produce a conjoining force. Nevertheless, both repulsive and attractive forces are embodied in the disjoining-pressure concept.

Derjaguin originally formulated the concept of a disjoining pressure for thin liquid films and was the first to verify experimentally its existence [7]. The more general and strict definition of the disjoining pressure given by Derjaguin and Churaev [8] is, 'In mechanical equilibrium the disjoining pressure, $\Pi(h)$, is equal to the difference existing between the component P_{zz} of the pressure tensor in the interlayer and the pressure, P_B, set up in the bulk of the phase from which it has been formed by thinning out:

$$\Pi(h) = P_{zz} - P_B = P_N - P_B. \tag{2.1}$$

In the simplest case of a one-component liquid phase, mechanical equilibrium under isothermic conditions implies thermodynamic equilibrium. In that case the disjoining pressure is a single-valued function of the interlayer thickness, h, ...'.

An example of how the pressure distributions P_N and P_T change in the thin-film region is provided in figure 3. The lengths of the horizontal arrows in figure 3 represent the magnitude of the pressure components while the direction (right or left) signifies the sign (positive or negative). For plane parallel films in equilibrium the normal component of the pressure tensor cannot change and remains constant through the film. Conversely, the tangential component can change in both sign and magnitude. However, beyond the transition zone, defined by δ in figure 3, $P_N = P_T$, and the pressure is isotropic and equal to the bulk pressure of the contiguous phases. A more detailed picture for a soap film stabilized by ionic surfactants is given by Eriksson and Toshev [9].

More recently, Kralchevsky and Ivanov have extended equation (2.1) and derive a general vectorial expression for the disjoining pressure [10, 11],

$$\Pi = \boldsymbol{n} \cdot (\boldsymbol{P} - P_R \boldsymbol{U})|_{r=r_0} \tag{2.2}$$

where $\boldsymbol{U}$ is the three-dimensional idemfactor, $\boldsymbol{P}$ is the total pressure tensor and $\boldsymbol{n}$ is an outer unit normal to the reference surface. r_0 corresponds to a reference surface dividing the film into two halves and P_R is a reference pressure. The utility of equation (2.2) is that it can be used for arbitrarily curved films without making model simplifications.

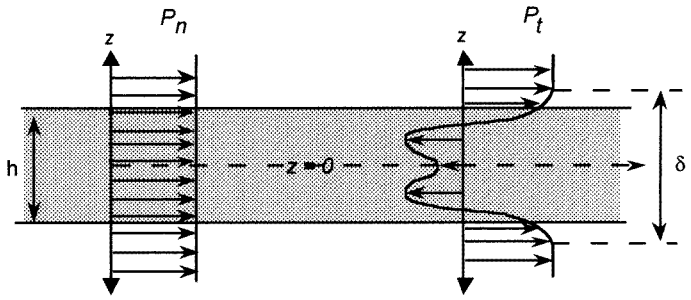

Figure 3. Typical distribution of the pressure tensor components P_N and P_T in a thin liquid film (after Derjaguin and Churaev [8]).

2.2. Thermodynamic definition

An alternative definition for the disjoining pressure can be formulated in terms of thermodynamic variables. In this case, the work required to change the thickness of a film at constant temperature T, overall pressure P, area A, and mole numbers N_i is expressed by a change in the Gibbs free energy of the film [9, 12],

$$\Pi(h) = -\left(\frac{\mathrm{d}G}{\mathrm{d}h}\right)_{T,P,A,N_i}. \tag{2.3}$$

For symmetrical foam films equation (2.3) can be used to generate the following familiar form of the Gibbs–Duhem relation for the film [6, 12–14]:

$$2\mathrm{d}\sigma = -s^f\,\mathrm{d}T - \Pi\,\mathrm{d}h - 2\sum_i \Gamma_i^f\,\mathrm{d}\mu_i \tag{2.4}$$

where σ is the surface tension, s^f is the excess entropy of the film interface and Γ_1^f and μ_i are the adsorption (i.e. surface excess concentration using the Gibbs convention) and chemical potential of the ith component. At constant temperature and chemical potential equation (2.4) reduces to the following useful relationship,

$$2\left(\frac{\mathrm{d}\sigma}{\mathrm{d}h}\right)_{T,\mu_i} = -\Pi. \tag{2.5}$$

Integration of equation (2.5) then yields an expression that relates the surface tension of the film interfaces to the disjoining pressure isotherm,

$$2\sigma(h) = 2\sigma(h=\infty) - \int_\infty^h \Pi\,\mathrm{d}h \tag{2.6}$$

where $\sigma(h=\infty)$ is the bulk value of the surface tension. In terms of the membrane model the equivalent expression is [6, 13, 14],

$$\sigma_f = 2\sigma(h=\infty) - \int_\infty^h \Pi\,\mathrm{d}h + \Pi h = 2\sigma(h=\infty) + \int_{\Pi(h=\infty)}^{\Pi(h)} h\,\mathrm{d}\Pi \tag{2.7}$$

where σ_f is the overall tension of the film and is used when all of the film properties are ascribed to a single two-dimensional plane. The latter two equations can be used to describe the effect disjoining forces have on film and three-phase contact angles [6, 14]. Thus these equations are the starting point towards developing bulk foam and emulsion constitutive equations which incorporate thin-film forces. When this is accomplished a clear correspondence between macroscopic properties, such as the contact angle at the Plateau border junctions of a foam, and thin-film interaction forces can be established.

3. Experimental measurements

Disjoining pressure isotherms are typically measured with a thin-film balance, TFB, based on the original design of Mysels and Jones [15]. Only a brief description of this device and the techniques to use it are given here; for a complete review the reader is referred to Claesson *et al* [16]. A schematic diagram of the experimental cell used is provided in figure 4. Single thin liquid foam (or emulsion) films are formed in the hole drilled through a fritted glass disc, onto which a glass capillary tube is fused. These solution-permeable film holders are placed in a gas tight measuring cell with the free end of the capillary tube exposed to a reference pressure (normally atmospheric pressure). Within the cell a precisely controlled capillary pressure is imposed on the film, which in equilibrium is balanced by the disjoining pressure.

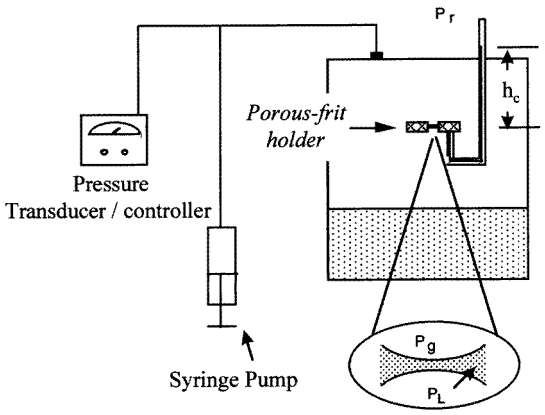

Figure 4. A schematic diagram showing the principal elements of a typical thin-film balance used to measure disjoining-pressure isotherms and monitor thin-film drainage.

This is accomplished by regulating the gas pressure in the cell with a syringe pump coupled to a pressure transducer/controller. As shown by Bergeron and Radke [17], this capillary pressure can be related to the disjoining pressure, Π, in a plane-parallel film by the following expression:

$$\Pi = P_g - P_r + \frac{2\sigma}{r} - \Delta\rho g h_c \tag{3.1}$$

where P_g and P_r are the gas and external reference pressures respectively, σ is the bulk surface tension of the solution, r is the radius of the capillary tube, $\Delta\rho$ is the density difference between the aqueous surfactant solution and the gas, h_c is the height of solution in the capillary tube above the film and g is the gravitational constant. Each term on the right side of equation (3.1) is measured independently, providing a direct measurement of Π.

Film thicknesses are conveniently measured using a variation on Sheludko's microinterferometric technique, in conjunction with video microscopy [5, 16, 17]. White light from a suitable source is passed through a heat filter and focused at normal incidence onto the individual foam film formed in the porous-plate holder. Reflected light from the film is then split and sent to a CCD video camera and a fibre optic probe placed in the microscope ocular. The video camera documents film drainage throughout the experiment while light from the fibre optic is filtered (e.g. $\lambda = 546$ nm) and analysed with a sensitive photon detection device (e.g. photomultiplier tube). The so-called 'equivalent' film thickness is then calculated from the standard Scheludko interferometric equation which assumes a constant refractive index across the film,

$$h_{eq} = \left(\frac{\lambda}{2\pi n_w}\right) \arcsin\sqrt{\frac{\Delta}{1 + 4R(1-\Delta)/(1-R)^2}} \tag{3.2}$$

where $\Delta = (I - I_{min})/(I_{max} - I_{min})$, h_{eq} is the equivalent film thickness, λ is the wavelength of light, $R = (n_w - 1)^2/(n_w + 1)^2$ and n_w is the refractive index of the surfactant solution. I is the instantaneous value of the reflected intensity while I_{max} and I_{min} correspond to the last interference maximum and minimum values. This equivalent thickness is slightly thicker than the true film thickness, h, because the surfactant adsorption layers at each film interface have a higher refractive index than the aqueous core. To correct for this difference the following

multilayer correction factors, derived by Duyvis, are commonly used [18]:

$$h = h_{eq} - 2h_{hc}\left(\frac{n_{hc}^2 - n_w^2}{n_w^2 - 1}\right) - 2h_{pg}\left(\frac{n_{pg}^2 - n_w^2}{n_w^2 - 1}\right) \tag{3.3}$$

where h_{hc} is the thickness of the surfactant hydrocarbon tails at the interface and h_{pg} is the surfactant's polar head-group thickness. These values can be calculated from the volume of the hydrocarbon chain and the polar head group, together with the area per molecule at the interface, which is evaluated from surface tension data using Gibbs' adsorption equation. n_{hc} and n_{pg} are the refractive indexes for the hydrocarbon tails and polar head groups. Finally, the thickness of the film's aqueous core, h_{aq}, can be determined by subtracting the thickness of the adsorbed layers from the total film thickness evaluated in equation (3.3),

$$h_{aq} = h - 2(h_{hc} + h_{pg}). \tag{3.4}$$

Disjoining-pressure isotherms are generated by measuring the equilibrium film thickness after applying a fixed capillary pressure to the film. Equilibrium conditions for most simple surfactant systems are reached after 10–90 minutes depending on the magnitude and change of the imposed capillary pressure. Systematic changes to the capillary pressure by altering the gas cell pressure, P_g, allow one to map out the entire repulsive (positive) branch of the disjoining-pressure isotherm (negative capillary pressures cannot be imposed with the porous-plate method). The disjoining pressures are then plotted against the film's aqueous core thickness, h_{aq}, to facilitate theoretical comparisons. The resulting disjoining-pressure isotherm is equivalent to the so-called surface-force curves generated from interactions between solid interfaces. Additional experimental details can be found elsewhere [16, 17].

4. Disjoining-pressure components

4.1. General approach

Changes in the interfacial region that generate the disjoining pressure in a thin liquid film originate from intermolecular forces. It is customary to separate the various contributions of the disjoining pressure into different components, e.g.,

$$\Pi(h) = \Pi_{dl} + \Pi_{van} + \Pi_{steric} + \Pi_{supra} + \cdots \tag{4.1}$$

where the subscripts in equation (4.1) indicate the following contributions: dl = electrostatic double-layer forces, van = London–van der Waals dispersion forces, st = steric and short-range structural forces (e.g., entropic confinement forces) and supra = forces arising from supramolecular structuring. Of course, models based on the application of equation (4.1) make the key assumption that the various contributions to the disjoining pressure are additive. However, it is not always clear that this assumption is valid and in some cases it may lead to anomalous results [19, 20].

Combination of the first two components listed in equation (4.1), Π_{dl} and Π_{van}, constitutes the well known DLVO theory. These two basic contributions are used throughout colloid science to describe particle interactions and provide the foundation for understanding colloid stability. Typically they are treated as separate and additive as suggested by equation (4.1), but Attard *et al* [19, 20] have recently extended classical Poisson–Boltzmann theory and show that the distinction made between van der Waals and double-layer forces is somewhat of an illusion. In addition, Attard *et al* incorporate the more complex behaviour that can occur due to 'image forces' and ionic correlations.

In what follows we briefly review each of the components in equation (4.1) separately for the purpose of highlighting the molecular origins of the disjoining pressure isotherm. For a comprehensive review several texts and monographs are available [3, 4, 21–23].

4.2. Electrostatic double-layer forces

One of the first and most studied contributions to the disjoining pressure arises from 'electrostatic' interactions. These interactions result from overlapping of the electric double layers that develop at charged interfaces. In the simplest case a repulsive force between the interfaces develops due to entropic confinement of the counter-ions which neutralize a charged interface. When the separation distance between two charged interfaces approaches twice the characteristic length for decay of the diffuse ionic atmospheres, λ, an additional external force is required to maintain the separation distance, as pictured in figure 5. From classical Debye–Hückel theory the characteristic length over which ions from a univalent electrolyte will act is given by [24]

$$\lambda = 1/\kappa = \sqrt{\frac{\varepsilon kT}{8\pi n^0 e^2}} \sim C^{-1/2} \tag{4.2}$$

where λ is called the Debye length, n^0 is the number density of ions, e is the elementary charge, ε is the dielectric constant of the medium, T is temperature, k is the Boltzmann constant and C is the concentration of electrolyte (moles l^{-1}). Equation (4.2) provides the important result that the decay length decreases as the electrolyte concentration increases (i.e. interactions become shorter range because of ionic screening).

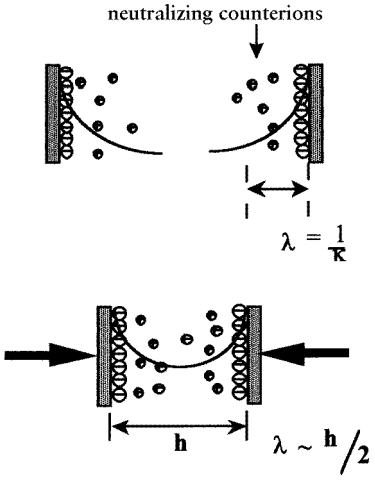

Figure 5. Two charged interfaces with their accompanying ionic atmospheres will interact when the separation distance, h, approaches twice the Debye length, λ.

The electrostatic double-layer forces are obtained by solving the Poisson–Boltzmann equation under a variety of different boundary conditions. There exists an extensive literature concerning the calculation of the electrostatic repulsion between interfaces [21–29], therefore, only two of the classic results will be given here as illustrative examples.

In most cases only relatively simple approximations for Π_{dl} are needed to capture the essential physics of double-layer interaction forces. Such approximations are typically valid for small surface charges where linearization of the Poisson–Boltzmann equation is acceptable. Under these conditions and assuming univalent electrolytes the constant surface potential and constant surface charge models for Π_{dl} are given by

Constant surface potential [21–25]

$$\Pi_{dl}^{\psi} = \frac{\varepsilon\psi_0^2}{8\pi}(\mathrm{sech}^2(\kappa h)) \tag{4.3}$$

Constant surface charge [21, 26, 27]

$$\Pi_{dl}^{\sigma} = \frac{2\pi\sigma_0^2}{\varepsilon}\left(\frac{1+\mathrm{sech}(\kappa h/2)}{\tanh(\kappa h/2)}\right)^2 \tag{4.4}$$

where ψ_0 is the potential and σ_0 is the charge density at the interface.

The constant surface potential model can be further simplified for large separation distances and small potentials to give the following well known form [22, 23]:

$$\Pi_{dl}^{\psi} = 64n^0kT\gamma^2\exp(-\kappa h)$$
$$\gamma = \left(\frac{\exp(Z/2)-1}{\exp(Z/2)+1}\right) \qquad Z = \frac{e\psi_0}{kT}. \tag{4.5}$$

Hunter [22] points out that under the conditions assumed, equation (4.5) is also valid for constant charge systems since little discharge occurs if the degree of double-layer overlap is small. More elaborate models for π_{dl} include charge regulation boundary conditions at the surface [28, 29] and effects due to ionic correlation and image forces [19, 20].

4.3. Dispersion forces

In addition to electrostatic double-layer forces London–van der Waals dispersion forces have long been recognized as being important in thin liquid films. The calculation of these forces has been approached in two different ways, microscopically and macroscopically.

The microscopic method, credited to Hamaker [30], came first and is based on pairwise summation of the individual dispersion interaction between molecules. Casmir and Polder [31] later supplemented this approach by including the correction for electromagnetic retardation. The molecular interaction potential used is typically represented by [32]

$$u(r) = -\frac{3}{2}\left(\frac{\overline{h}\nu_1\overline{h}\nu_2}{\overline{h}\nu_1+\overline{h}\nu_2}\right)\frac{\alpha_1\alpha_2}{r^6} \tag{4.6}$$

where $u(r)$ is the interaction potential between two spherically symmetric molecules, 1 and 2. $\overline{h}$ is Planck's constant, ν_i is a characteristic electronic frequency for each molecule in its unexcited state and α_i is the polarizability of molecule i. In order to obtain the force of interaction between two macroscopic bodies equation (4.6) is integrated over the volume of the system, which for two plane-parallel surfaces separated by a vacuum gap yields [23, 30]

$$\Pi_{van} = -\frac{A_{12}}{6\pi h^3} \tag{4.7}$$

where A_{12} is known as the Hamaker constant. At large separations retardation effects (finite response time of the induced dipoles) can become important, and lead to a decreased interaction that decays faster ($\Pi_{van} \sim 1/h^4$) [31]. When the interaction between two different bodies, 1 and 2, is mediated by a third phase, 3 (e.g., aqueous films 3 sandwiched between phase 1 and phase 2) the potential energy of interaction, Ω_{132}, becomes

$$\Omega_{132} = A_{132}\iint\frac{\mathrm{d}V_1\,\mathrm{d}V_2}{r^6} \tag{4.8}$$

where

$$A_{132} = (A_{12} + A_{33} - A_{23} - A_{13})$$

and V_i corresponds to the volume of phase i and A_{132} is the composite Hamaker constant. Like the electrostatic component many elaborate models have been developed to handle different geometries and more complex systems (e.g. multilayered films) [18, 23, 33, 34].

The fundamental shortcoming of the microscopic approach stems from the assumed pairwise additivity of the molecular interactions. However, this problem is overcome if we adopt an alternative point of view and consider the interacting bodies as a continuous media. This macroscopic approach was developed by Lifshitz [35, 36] and the theory now bears his name. The basic idea of the theory is that the interaction between the bodies is considered to take place through a fluctuating electromagnetic field. In this approach the fields are calculated on the basis of the exact Maxwell equations, so that the effects of retardation, caused by finite propagation velocities of the electromagnetic waves, are automatically taken into account. The Lifshitz result for a thin uniform film of phase 3 between two semi-infinite phases, 1 and 2, is given by [35–37]

$$\Pi_{van} = \frac{\bar{h}}{2\pi^2 c^3}\int_0^\infty\int_1^\infty p^2\xi^2\varepsilon_3^{3/2}\left\{\left[\frac{(s_1+p)(s_2+p)}{(s_1-p)(s_2-p)}\exp\left(\frac{2p\xi}{c}h\sqrt{\varepsilon_3}\right)-1\right]^{-1}\right.$$
$$\left.+\left[\frac{(s_1+p\varepsilon_1/\varepsilon_3)(s_1+p\varepsilon_2/\varepsilon_3)}{(s_1-p\varepsilon_1/\varepsilon_3)(s_2-p\varepsilon_1/\varepsilon_3)}\exp\left(\frac{2p\xi}{c}h\sqrt{\varepsilon_3}\right)-1\right]^{-1}\right\}\mathrm{d}p\,\mathrm{d}\xi \qquad (4.9)$$

where

$$s_1=\sqrt{\varepsilon_1/\varepsilon_3-1+p^2} \qquad s_2=\sqrt{\varepsilon_2/\varepsilon_3-1+p^2} \qquad c=\text{speed of light}$$

and ε_1, ε_2 and ε_3 are functions of imaginary frequency $\omega = \mathrm{i}\xi$. However, the quantity $\varepsilon(\mathrm{i}\xi)$ is a real function that can be evaluated from

$$\varepsilon(\mathrm{i}\xi) = 1+\frac{2}{\pi}\int_0^\infty \frac{\omega\varepsilon''(\omega)}{\omega^2+\xi^2}\,\mathrm{d}\omega. \qquad (4.10)$$

$\varepsilon''(\omega)$ is the imaginary part of the dielectric response function and $\omega\varepsilon''(\omega)$ measures the spontaneous electric field fluctuations in a body as well as a substance's ability to dissipate applied electrical energy [22, 37].

Needless to say equation (4.9) is a bit cumbersome and its original derivation is rather lengthy. However, many subsequent treatments of the macroscopic theory are now available which provide both a more readily understandable approach and many useful approximate expressions [22, 23, 37]. In fact, using the method of Parsegian and Ninham [37, 38] to determine the dielectric response function (equation (4.10)) from absorption data and reflectance measurements, it is now quite straightforward to calculate dispersion forces from Lifshitz's theory.

Although the macroscopic approach is a great improvement over the classical Hamaker summations, it is not expected to hold when a film becomes so thin that its dielectric properties change with thickness or when molecular orientation is important. This can be an important consideration for aqueous films that undergo structuring near the interface.

4.4. Steric (entropic) forces

Entropic confinement forces are a third class of forces that occur in ultrathin surfactant films (<5.0 nm) and between bilayers in solution. Π_{steric} is introduced into equation (4.1) to cover contributions to the disjoining pressure that are responsible for the stability observed in so-called Newton black soap films (see figures 6 and 7). In concept this component is similar to the 'adsorption component of disjoining pressure' introduced by Derjaguin *et al* [21], that arises from the steric repulsion occurring when adsorbed layers overlap. More recently, Israelachvili and Wennerström [39] have outlined the physical origin of these forces more precisely and have

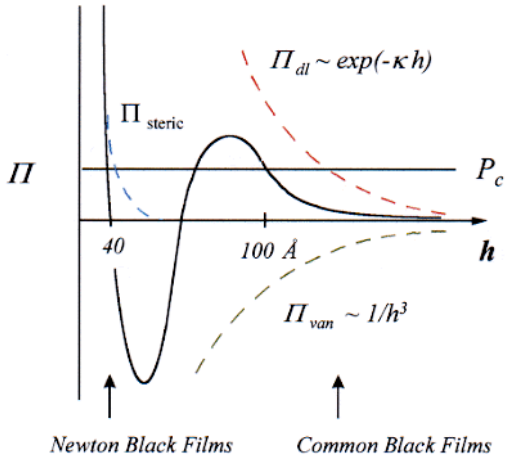

Figure 6. Schematic representation of a disjoining-pressure isotherm that includes contributions from Π_{dl}, Π_{van} and Π_{steric}.

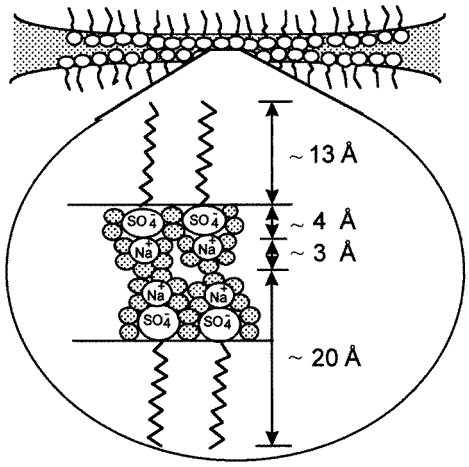

Figure 7. Schematic diagram showing the profile of a Newton black film of sodium dodecyl sulphate. Filled circles correspond to water in the first hydration shell, surfactant head groups are labelled and the hydrocarbon chain is depicted by the irregular lines.

carefully categorized the various modes by which they operate. The general classifications given by them include:

Undulation—forces created by undulations of the interface (inversely proportional to the bending modulus, K_b, $\Pi_u \sim 1/K_b$).

Peristaltic—forces generated by peristaltic fluctuations as two fluid interfaces approach (inversely proportional to the compressibility modulus, K_a, $\Pi_p \sim 1/K_a$).

Head-group overlap—a steric stabilization force that becomes important in systems containing large nonionic headgroups. These forces can be described by theories used for polymer 'brushes'.

Protrusion—molecular scale protrusions of surfactant molecules at the interface. Π_{pro} can be approximated from [39]

$$\Pi_{pro} = \frac{n\beta(h/\zeta)\exp(-h/\zeta)}{[1-(1+h/\zeta)\exp(-h/\zeta)]} \tag{4.11}$$

where $\zeta = kT/\beta$ is the protrusion decay length, n is the density of protrusion sites and β is an interaction parameter (J m^{-1}).

A semiquantitative treatment of these entropic confinement forces is presented by Israelachvili and Wennerström in their review.

Also important in extremely thin films are solvation forces [23], or, when water is the solvent, hydration forces. These forces originate from molecular ordering at the interface. When two interfaces approach this ordering is disturbed, resulting in forces of attraction and repulsion. These short-range interactions can be very complex and depend on how the molecules structure at an individual surface, then how this structure is modified once a second surface is encountered. The simplest liquids display force curves that oscillate with a periodicity equal to the liquid's molecular diameter and can be modelled by treating the molecules as hard spheres between two hard walls [23]. Water, however, has strong dipoles that can lead to hydrogen bonding and long-range dipole polarization. These effects generate repulsive 'hydration' or attractive 'hydrophobic' interactions in addition to the short-range oscillatory interaction.

Figure 6 shows a schematic of a foam film disjoining-pressure isotherm which includes the entropic force contributions, Π_{steric}, superimposed on the classical DLVO components, Π_{dl} and Π_{van}. It is important to note that thermodynamically metastable films can exist only in negatively sloping regions of the isotherm. Hence, the portion of the curve with a positive slope separates the isotherm into two metastable regions, thick ($\sim$50 nm) common black films (CBFs) and thinner ($\sim$4 nm) Newton black films (NBFs). In foam, CBF stability is normally due to the electric double-layer forces while NBF stability is not as well understood but can be accounted for by the short-range entropic confinement forces outlined above.

X-ray reflectivity experiments [40] and molecular dynamic calculations [41] confirm the schematic representation of the NBF pictured in figure 7. In this figure the filled circles represent water molecules in the first hydration shell that surround the polar head groups of sodium dodecyl sulphate (SDS) surfactant molecules adsorbed to an air–water interface. The hydrocarbon chain of the surfactant (i.e. surfactant tails) are indicated by the irregular lines that extend out of the aqueous film region. Approximate thicknesses have been indicated and from the picture it is clear that very little space is left for unbound water and the interior of the NBF film resembles a solid-like structure.

4.5. Common black film stability

The disjoining-pressure isotherm in figure 6 represents the energy barrier referred to in our earlier discussions concerning the long-term stability of films (see also figure 2). From these discussions it should be evident that when an external capillary pressure in excess of the maximum disjoining pressure is applied to the film, we will breach the energy barrier holding the film in its metastable state and film rupture can occur. However, a classical DLVO approach, which simply balances repulsive and attractive interactions across the film to gauge the magnitude of the energy barrier, can not fully explain the film stability behaviour witnessed in foam and emulsion systems.

Recently, certain limitations of applying classical DLVO concepts to foam and emulsion films have been revealed [42]. Unfortunately a classical DLVO force analysis of film rupture

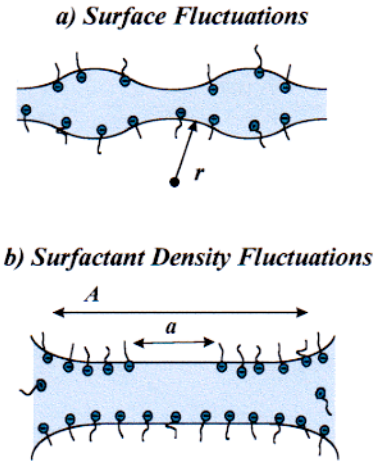

Figure 8. Schematic diagrams of the spatial and surfactant density fluctuations in thin liquid films: (a) a typical spatial fluctuation; (b) a local depletion zone due to monolayer density fluctuations.

treats the film surfaces as solid uniformly charged non-deforming walls; however, foam and emulsion films have both spatial and surfactant density (i.e. charge) fluctuations occurring at the interface. In reality these fluctuations are superimposed on one another, but for clarity the schematic diagrams in figures 8(a) and (b) depict the two cases separately. Since film rupture (and/or a thickness transition) from a metastable state is essentially a nucleated 'wetting phase transition', fluctuations can be important near the phase spinodal, as with bulk phase transitions near the critical point. Using simplified analyses one can discover useful insight into which processes and system parameters are important for controlling the fluctuations not accounted for in DLVO theory.

The original work of Vrij [43, 44] has spawned considerable attention concerning the effect spatial fluctuations have on the *spinodal decomposition* of unstable film states; however, the early work of De Vries [45] seems to be one of the few that addresses *nucleated* rupture of rather thick foam films (i.e. CBFs). Likewise, understanding how surfactant density fluctuations might directly affect the DLVO forces and metastability of foam and emulsion films has received very little attention. We note that nucleated rupture of ultra-thin NBF films has been treated, but these films do not undergo thickness variations and are essentially molecular leaflets for which the repulsive disjoining forces are not as well understood. Thus, for NBF films it is not clear whether continuum concepts apply (i.e. surface tension etc) and the activation energy for film rupture may be governed by different physical parameters [46–48].

Considering the simple disjoining-pressure isotherm in figure 9 helps to understand within the framework of familiar DLVO concepts which film properties control the fluctuations responsible for overcoming the energy barriers that hold a simple CBF in its metastable state. The solid curve in figure 9 represents a typical DLVO profile for a system trapped in a metastable energy minimum at a particular imposed capillary pressure. The dashed lines and curves in the figure correspond to how fluctuations influence the disjoining pressure maximum, $\Delta\Pi_{max}$, and variations in the applied capillary pressure, ΔP_c. As with the standard DLVO premise, when the applied pressure exceeds the disjoining pressure the film has overcome the barrier trapping the film in a local thermodynamic minimum. After this point is reached the spinodal decomposition analysis of Vrij [43, 44] describing the lifetime of a thermodynamically unstable film is formally applicable. The point to be made is how fluctuations can promote this unstable stage.

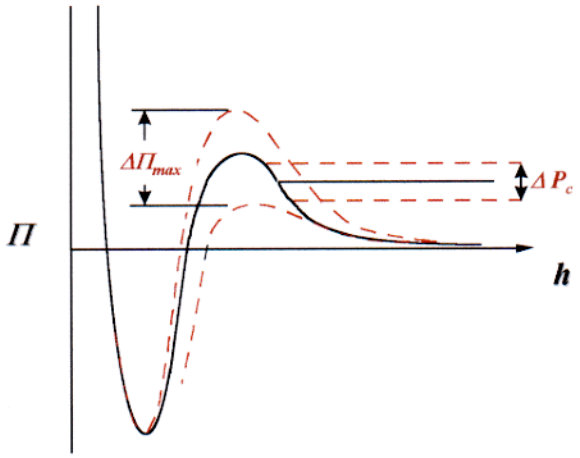

Figure 9. A schematic diagram depicting how fluctuations in the capillary pressure, ΔP_c, and the disjoining pressure, $\Delta\Pi_{max}$, influence the local barrier height relative to the imposed capillary pressure along the film.

4.5.1. Spatial fluctuations. The spatial fluctuations shown in figure 8(a) manifest themselves as pressure fluctuations along the film, ΔP_c in figure 9. The probability of a certain fluctuation depends on the energy expended to create it,

$$P_s \sim c_s \exp\left(-\frac{\Delta G_s}{kT}\right) \tag{4.12}$$

where P_s is the probability of the spatial fluctuation, c_s is a constant and ΔG_s is the energy expended. For a pure fluid, a simple one-dimensional energy analysis for a sinusoidal fluctuation of the type pictured in figure 8(a) was worked out by Vrij and Overbeek [44]. When surfactant is present, Bergeron has shown that ΔG_s becomes [42]

$$\Delta G_s = (\varepsilon + \sigma)\frac{2B^2\pi^2}{\Lambda} - \Lambda B^2 \frac{\mathrm{d}\Pi}{\mathrm{d}h} \tag{4.13a}$$

$$\varepsilon = \frac{\mathrm{d}\sigma}{\mathrm{d}\ln a} = \varepsilon_d + \mathrm{i}\eta_s\omega \tag{4.13b}$$

where ε is the surface dilatational modulus, ε_d and η_s the elastic and shear dilational moduli, ω the frequency of the disturbance (we note $\varepsilon_d \sim \varepsilon_0$ when $\omega \sim \infty$), B the amplitude of the disturbance and Λ its wavelength. The second term in equation (4.13*a*) accounts for the change in interaction energy accompanying the disturbance and is normally a small contribution to the overall energy change [45]. The difference between equations (4.13) and Vrij's classical expression is the surface modulus term which arises from having surfactant adsorbed to the interface. Higher-order surface curvature terms can also be incorporated into the analysis but they are typically small in comparison to ε and σ [49]. Since the surface modulus (i.e. elasticity) may in some cases exceed the surface tension, it can actually become the most influential contribution to the disturbance. Hence, with reference to equation (4.12) we see that high surface moduli decrease the probability of the disturbance (i.e. *dampen spatial fluctuations*). The hydrodynamic influence associated with this surface modulus effect is often qualitatively expressed as a Gibbs–Maringoni stabilization mechanism. Long ago Lucassen-Reynders and Hansen demonstrated experimentally that surfactant monolayers do indeed have a strong dampening effect on surface fluctuations [50].

The film size can also have an influence on the energetics of the spatial fluctuations. This effect was originally identified by Vrij and is revealed in equations (4.13) by scaling the film diameter with the wavelength of the disturbances. In summary, for very small films Λ will be restricted by the film diameter and consequently only short wavelength disturbances are possible. Thus, when the film dimensions restrict the wavelength for a disturbance, a fixed amplitude wave will expend more energy and the disturbance will be less probable in these wavelength restricted films. That is, small metastable CBF films should be less susceptible to spatial fluctuations and hence show an increased stability. The actual film size where this becomes important depends on the system; however, Vrij has shown that spatial fluctuations can be significantly dampened in micron sized films [43, 44].

4.5.2. Surfactant density fluctuations. Interfacial surfactant density fluctuations, figure 8(b), are another factor not accounted for in a classical DLVO description of thin-film forces. For ionic surfactants these fluctuations induce charge fluctuations which in turn can influence the local height of the DLVO barrier, $\Delta\Pi_{max}$. An analogous study showing how a fluctuating barrier height increases particle coagulation kinetics indicates that surfactant density fluctuations may also be important in the rupture process of foam and emulsion films [51–53]. Applying a standard statistical thermodynamic approach to the interface provides a simple method for investigating which properties influence surfactant density fluctuations at the air–water interface [42]. Analogous to bulk density fluctuations, surface density fluctuations can be expressed by

$$\frac{\langle(\Delta\Gamma)^2\rangle}{\langle\Gamma\rangle^2} = \frac{kT}{\Gamma^2 a}\left(\frac{\mathrm{d}\Gamma}{\mathrm{d}\mu}\right)_T \tag{4.14}$$

where the right-hand side of equation (4.14) represents the mean square relative deviation from the mean of the surfactant adsorption, μ is the chemical potential and a is the area over which the surface fluctuation is considered. In addition, surface thermodynamics provides the following relation:

$$\left(\frac{\mathrm{d}\Gamma}{\mathrm{d}\mu}\right)_{T,N} = \frac{\Gamma^2}{\varepsilon_0}.$$

Substitution of this expression into equation (4.14) reveals a direct analogy between the role played by the surface elasticity (i.e. Gibbs elasticity) and the bulk compressibility in modulating density fluctuations.

Adsorption density fluctuations

$$\frac{\langle(\Delta\Gamma)^2\rangle}{\langle\Gamma\rangle^2} = \frac{kT}{\varepsilon_0 a}. \tag{4.15a}$$

Bulk density fluctuations

$$\frac{\langle(\Delta\rho)^2\rangle}{\langle\rho\rangle^2} = \frac{kT\kappa}{v}. \tag{4.15b}$$

Here ρ represents the bulk density, κ is the bulk compressibility factor and v the volume. This analogy demonstrates the notion that compressibility is inversely related to elasticity.

Finally, we can express the probability of having a given fluctuation, P_Γ, by

$$P_\Gamma \sim c_\Gamma \exp\left(-\frac{\Delta\Gamma^2}{2\langle\Delta\Gamma^2\rangle}\right)$$

and with the help of equation (4.15*a*) we find that the probability of exposing a bare surface of size a, as depicted in figure 8(b), becomes

$$P_\Gamma \sim c_\Gamma \exp\left(-\frac{\varepsilon_0 a}{kT}\right). \tag{4.16}$$

The charge fluctuations associated with the surfactant density fluctuations described by equation (4.16) will likely become important when a is of the order of the film thickness and when the time scale for film rupture (or transition) is close to that of the fluctuation period. Important to note from equation (4.16) is that high surface elasticities will diminish the probability of surfactant density fluctuations and thus produce films less sensitive to this phenomenon.

Although equations (4.12) and (4.16) are somewhat qualitative and only consider thermally induced fluctuations, they do provide important physical insight concerning film rupture. Both equations indicate that the surface elasticity plays a key role in dampening both spatial and density fluctuations in foam and emulsion films. When these fluctuations are dampened the probability of overcoming the activation barrier which holds a film in a metastable state is lower and the film will be more stable. Equations (4.12) and (4.16) solidify the intuitive notion that not only is the height of the activation barrier important, but also the system's ability to resist disturbances. In addition, these simplified expressions provide a clear picture of how the surface elasticity influences the energetics of the film-rupture process. Whether or not disturbances are thermally or mechanically induced a cohesive surfactant monolayer with a high surface elasticity will promote film stability.

4.6. Hydrophobic forces

It is now well established that a long-range (>10 nm) attractive force operates between hydrophobic surfaces immersed in water and aqueous solutions [54]. This force can be much stronger than those predicted on the basis of van der Waals interactions and is termed the hydrophobic force. So far no generally accepted theory has been developed for these forces, but the hydrophobic force is thought to arise from overlapping solvation zones as two hydrophobic species come together [23]. In fact, Eriksson *et al* [55] have used a square-gradient variational approach to show that the mean field theory of repulsive hydration forces can be modified to account for some aspects of hydrophobic attraction. Conversely, Ruckenstein and Churaev suggest a completely different origin that attributes the attraction to the coalescence of 'vacuum gaps' at the hydrophobic surfaces [56]. The exact origins and character of the hydrophobic attraction remains an open question that is currently the subject of extensive research.

4.7. Supramolecular forces

Relatively new types of forces, due to supramolecular structuring of amphiphilic molecules, within foam films have been recently measured [17]. Moreover, several works dating from the turn of the century have demonstrated film-thinning phenomena (commonly referred to as film stratification) that arise from supramolecular forces [57–60]. In addition and independently the same type of structural force between surfactant coated crossed mica cylinders in a surface-force apparatus have been observed [61, 62]. The general form of the force curves obtained for these systems is summarized in figure 10.

In systems studied thus far the forces can be extremely long range (>50 nm) and oscillatory, having a periodicity set by the *effective* size of the structures responsible for the forces. The most common occurrence of supramolecular structural forces in thin films is when relatively high concentrations of surfactant are present in a system. In such systems a variety of structures

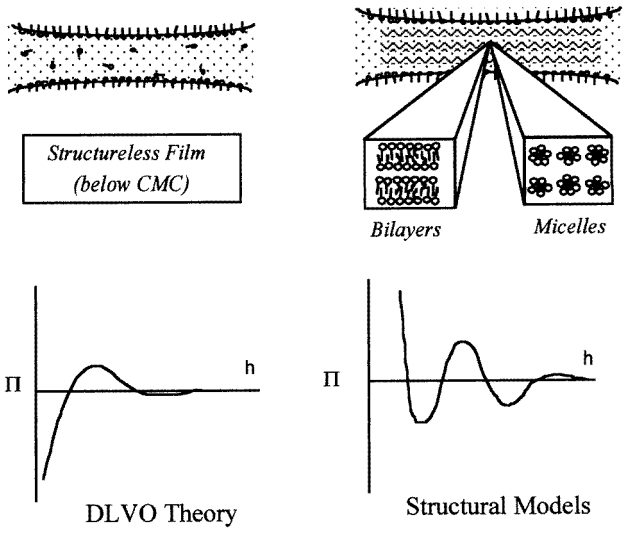

Figure 10. The general form of the force curves for systems with and without supramolecular structuring. Only two types of structure are depicted; however many different types can occur depending on the system.

can form depending on the nature and composition of the amphiphile in the system, ionic strength, and external conditions such as temperature. Therefore modelling supramolecular forces typically requires assumptions about the structures that are present in the film. The two most frequently encountered structures in thin liquid soap films are repeating units of surfactant bilayers [63–65] or ordered arrays of micellar domains [66, 67].

4.7.1. Micellar structural forces. Mysels was the first to suggest that micelles can contribute to the disjoining forces in foam films [68, 69]. Since then attempts have been made to model this effect [67, 70]. The first treatment describing this phenomenon within a thermodynamic framework is by Pollard and Radke [67], who utilize density functional theory (DFT) to calculate a micellar contribution to the disjoining pressure, Π_{mic}. This method sums the force exerted on the interfaces by the micelles in the film:

$$\Pi_{mic} = -\frac{1}{2}\int_0^h \rho(x;h)\left[\frac{\mathrm{d}U_{m-1}(x)}{\mathrm{d}x} + \frac{\mathrm{d}U_{m-2}(h-x)}{\mathrm{d}x}\right]\mathrm{d}x - P_B \qquad (4.17)$$

where x defines the location in the film, U_{m-i} is the interaction potential between a micelle and interface i, and P_B is the reference bulk pressure of the fluid in equilibrium with the film. $\rho(x;h)$ is the number density distribution of micelles in the film which is obtained from variational differentiation of the Helmholtz free energy, F, with respect to $\rho(x;h)$,

$$\frac{\delta F[\rho(x)]}{\delta\rho(x)} = -\mu + U^{ext} \qquad (4.18)$$

where μ is the chemical potential and U^{ext} is the external potential (i.e. a typical DLVO-type potential). Calculations using equation (4.17) show that charged micelles have energetically preferred locations within the film which cause them to create a micellar density profile that has an oscillatory form. Thus the density distribution of micelles in the film forms a series of peaks that define the most probable position of finding a micelle in the interior of the film (see figure 11). As the film thickness decreases micelles are 'squeezed' out of the film and

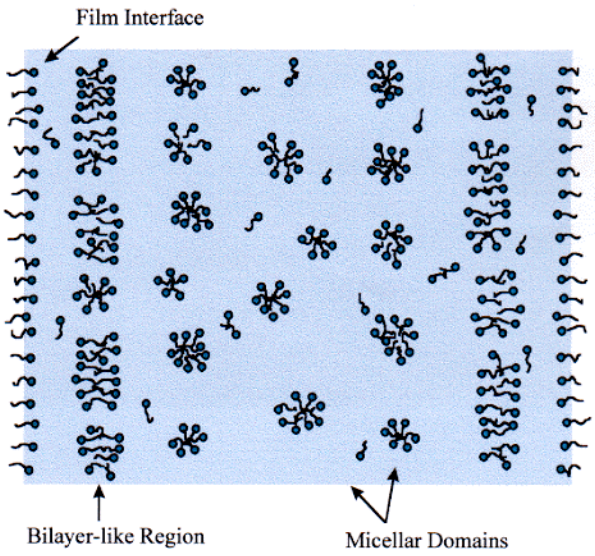

Figure 11. Schematic representation of supramolecular ordering that can occur in concentrated micellar solutions. Depending on the solution conditions structural changes in the high-concentration zones near the interface can take place.

the number of density peaks decreases concomitantly. Since the micelle structuring generates multiple values of the film thickness that are thermodynamically unstable ($\partial\Pi/\partial h > 0$), the squeezing out process occurs in a discrete manner, changing from one stable configuration to the next. That is, DFT allows us to interpret the oscillatory branches of the force curve as arising from micellar structuring in the film via a local thermodynamic minimum set up at different film thicknesses, not kinetic trapping as originally postulated [70].

One important point concerning forces generated by micellar structuring is the difference in the magnitude of the forces found between SFA measurements and those obtained for foam films. In foam films the magnitudes are low, of the order of 100 Pa, while SFA measurements on similar systems exceed 10^4 Pa. This difference most likely comes from physical differences between the interfaces in the two experiments. SFA measurements confine a fluid between two solid interfaces, which support more stress and have much lower levels of fluctuations compared to fluid interfaces. Thus solid interfaces can promote a higher degree of supramolecular order. The calculations of Pollard and Radke are consistent with this fact. Conversely, a fluid interface is flexible and can absorb energy through deformations (bending modes) which will diffuse the ordering between the interfaces. The spatial and density fluctuation effects on the measured forces and metastable states of 'stratifying' foam and emulsions films are similar to the discussion provided in section 4.5 of this review.

4.7.2. Bilayer and lamellar structural forces. Clearly different types of molecular structuring in addition to micellar (e.g. bilayer, liquid crystal) can occur and modelling these systems in foam films has received little attention. However, Perez *et al* [71, 72] have developed a theory for the structural component of the disjoining pressure in thin films of liquid crystals. Their thermodynamic theory is based on the concept of surface tension anisotropy (i.e. variation of nematic liquid crystal interfacial tension with molecular orientation at the interface). The primary contributions to the force results from a balance of two torques:

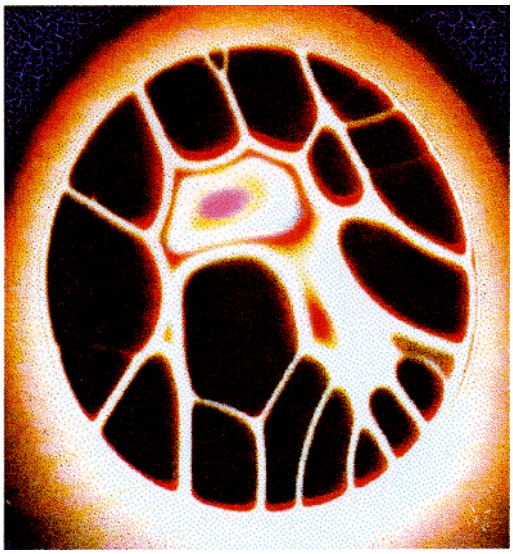

Figure 12. An interference microscope image of a 0.2 cm foam film containing a microtubular network embedded in the film.

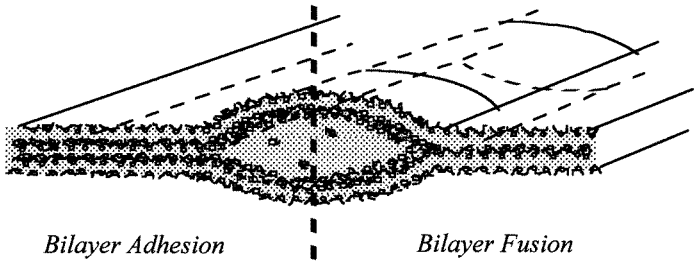

Figure 13. Cross-sectional view of the proposed general molecular structure of an embedded microtube that consists of two wrinkled bilayers sandwiched in a foam film. Features such as the number of bilayers composing a tube and whether or not bilayer adhesion or fusion is operative remain to be verified.

τ_{el}: elastic torque opposing disalignment of molecules
τ_s: surface torque opposing an increase of surface free enthalpy or surface tension.

For more dilute systems (e.g. vesicular solutions) thin films containing highly flexible bilayers can be obtained [73]. In this case bilayer undulation forces (so-called 'Helfrich forces') as described in section 4.4 can play a role. These forces are repulsive and originate from the entropic confinement of bilayers in a film. Although in some cases good agreement is found between theory and experiment, there still remain many unexplored problems that should prove to be both challenging and exciting problems for future research.

The most recent experimental work on bilayer containing films has also revealed new hydrodynamic phenomena that may prove important for understanding biological membrane interactions [73]. An example of the fascinating hydrodynamic behaviour that is observed when two bilayers fuse or adhere within an individual foam film is pictured in figure 12. This figure contains a photographic image of a single foam film which is 0.2 cm in diameter. The dark regions in the photograph correspond to a uniform 10 nm thickness film while the light

and coloured regions range from 100 to several hundreds of nanometres thick. Thus, the long interconnected strands running through the film are actually thick-film regions (microtubes) suspended in the film. The formation of these tubular regions resembles the formation of wrinkles in freshly deposed wall-paper. That is, excess material is pushed together and eventually trapped to form a wrinkle. In the present case the wrinkles are composed of fused bilayers as sketched in figure 13. The entire process is directly analogous to the 'pockets' of excess fluid created during the membrane binding transition seen for lipid bilayers [74, 75]. Further details can be found elsewhere [73].

4.7.3. Structures and forces in polymer and polymer/surfactant containing films. Some of the newest force/structure relationships within thin films have been found when soluble polymers are added to a system [76]. Whether or not low-molecular-weight surfactants are present or not, polymer (and protein) containing systems reveal many different thin-film properties. As most practical systems do contain both surfactants and polymers we have sketched in figure 14 a summary of the four most commonly seen adsorption/complexation interactions that occur between various mixtures of the two. This general summary is clearly not exhaustive but as these situations often arise it is convenient to identify the general categories as (I) *repulsion/exclusion*, (II) *synergistic adsorption*, (III) *surface depletion* and (IV) *indifferent adsorption*. Case (I), repulsive interactions, can occur when polyelectrolytes carry the same charge as an ionic surfactant, while case (II) is often encountered with oppositely charged polyelectrolyte/surfactant mixtures. Case (III) takes place for surfactants that have a strong hydrophobic interaction with the polymer and the resulting complex becomes less surface active. Case (IV) is rarer and requires very weak interactions between the polymer and surfactant. It should also be noted that the various situations dependent on the relative concentrations of the different components and one particular chemical system can change its behaviour depending on the solution composition. The reader is referred to Goddard and

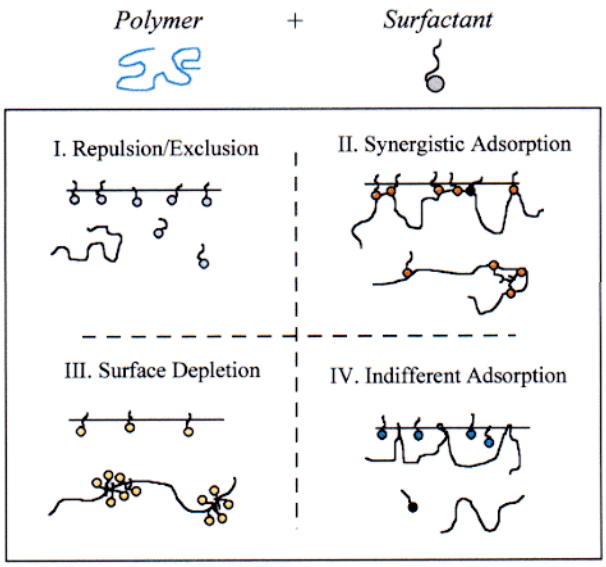

Figure 14. A summary of the four most commonly seen adsorption/complexation interactions that occur between various mixtures of polymers and surfactants.

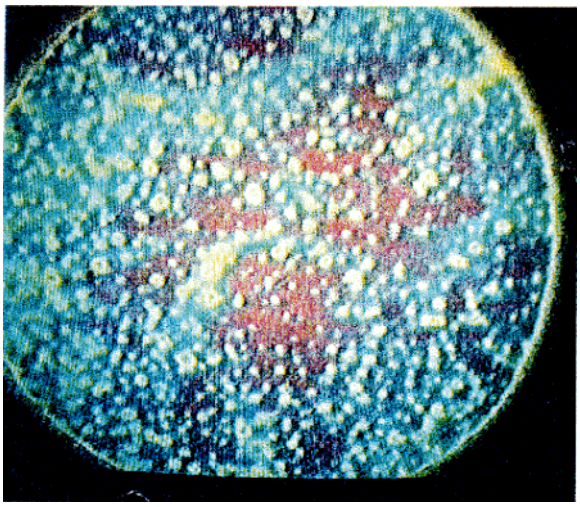

Figure 15. An interference microscope image of a foam film stabilized by adsorbed polymer/surfactant complexes that create a gelled network within the film. Different colours correspond to different film thicknesses (see text for details).

Ananthapadmanablan [77] for a detailed review of polymer/surfactant interactions and their adsorption to interfaces.

Quantitative thin-film force measurements of polymer/surfactant containing systems is just beginning and already quite fascinating behaviour has been found [76]. In particular the strongly interacting synergistic adsorption system (e.g. case (II)) containing an anionic polyelectrolyte and a cationic surfactant has been extensively studied. This system has revealed both oscillatory force versus distance profiles and interfacial gel formation within individual films.

At relatively low polymer adsorption, oscillatory force profiles similar to those observed for micellar solutions are also seen in polyelectrolyte containing systems. Like micellar structuring, these oscillations originate from an inhomogenous density distribution of polymer (or polymer/surfactant complexes) within the film. Furthermore, the characteristic length scale of the oscillatory forces indicate that this structuring is controlled by electrostatic interactions. To date no complete theory describing this phenomena exists; however Monte Carlo simulations of confined polyelectrolytes in thin films clearly predict non-homogeneous density profiles and oscillations in the force–distance isotherms [78–80]. These simulations lead to the interpretation that force oscillations will arise when the chains from one density rich region are forced close enough to sample an adjacent high-density region. At this point the two regions merge to occupy the same 'coulombic well', resulting in a discrete jump in film thickness and expulsion of any excess polymer. Experimentally these coulombic wells are found to be separated by the characteristic correlation distance, ξ, found in the bulk solution. The process was originally expressed as 'polymer bridging' [78, 79], but this type of bridging should not be confused with bridging that involves polymer adsorption; the present case is simply a *fusion of density rich polymer regions* which is analogous to the fusion of micelle rich regions that generate similar oscillatory force profiles in concentrated surfactant solutions, see section 4.7.1.

When there is high polymer (or polymer/surfactant complex) adsorption onto a fluid interface a thin film containing a gel-like network can be created when two such interfaces are brought into contact. An example of these gelled films can be found in figure 15. The film

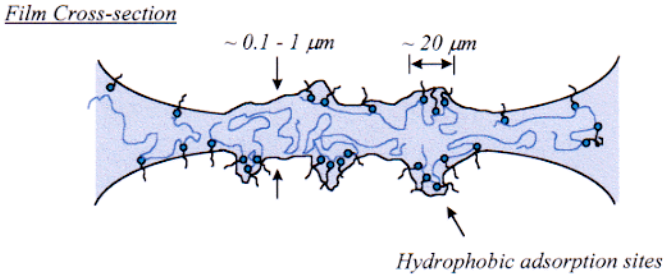

Figure 16. Typical cross-sectional view of a film containing a gel-like network of adsorbed polymer/surfactant complexes.

pictured in figure 15 is much thicker than common soap films as can be seen by the strong iridescent colours it produces via thin-film interference under white light illumination. Each colour corresponds to a different film thickness and it is evident that the thickness is highly heterogeneous throughout the film. In fact there are two types of heterogeneity: microscopic, on the order of 20 μm diameter, which appear as spots scattered throughout the film, and much larger irregularly shaped macroscopic domains. A schematic diagram of a typical film cross section deduced from figure 15 is shown in figure 16. Although the general features of these gelled films are highly reproducible, it should be noted that the structures formed are not equilibrium structures and their form and properties depend on the rate of film formation. When films are formed quickly the polymer chains extending from the surface do not have time to rearrange into an equilibrium configuration and thus they become trapped (quenched) into a complicated network of knotted overlapping adsorption layers. Furthermore, unlike solid surfaces, thin liquid films have highly deformable interfaces that succumb to the local pressures generated by squeezing the entangled polymer network. Surface tension forces are not strong enough to prevent this deformation, thus these films develop a very heterogeneous thickness profile. This deformation results in a distribution of energy which has not been considered in previous surface force theories, hence standard polymer interaction theories between flat surfaces cannot be applied to these systems. It is clear that the gel-like films described here play an important role in film stabilization and various other thin-film properties, thus the complex behaviour seen with these systems remains one of the many exciting areas for future work.

Acknowledgment

The author wishes to thank Rhône-Poulenc for the opportunity to publish this work.

References

[1] Hooke R 1757 Communicated to the Royal Society, March 1672 *The History of the Royal Society of London* vol 3, ed T Birch (London) p 29
[2] Newton I 1952 Book II, Obs. 17–19 *Opticks, Based on the 4th ed. London 1730* (New York: Dover) pp 214–19
[3] Derjaguin B V 1989 *Theory of Stability of Colloids and Thin Films* transl. R K Johnston (New York: Consultants Bureau)
[4] Verwey E J W and Overbeek J Th G 1948 *Theory of the Stability of Lyophobic Colloids, the Interaction of Sol Particles Having and Electric Double Layer* (collaboration with K Van Nes) (New York: Elsevier)
[5] Scheludko A 1967 *Adv. Colloid Interface Sci.* **1** 391
[6] Ivanov I (ed) 1988 *Thin Liquid Films, Fundamentals and Applications* (New York: Dekker)

[7] Derjaguin B and Obuchov E 1936 *Acta Phys. URSS* **5** 1–22
[8] Derjaguin B and Churaev N V 1978 *J. Colloid Interface Sci.* **66** 389
[9] Eriksson J C and Toshev B V 1982 *Colloids Surf.* **5** 241
[10] Kralchevsky P A and Ivanov I B 1990 *J. Colloid Interface Sci.* **137** 234
[11] Kralchevsky P A and Ivanov I B 1988 Mechanics and thermodynamics of curved thin films *Thin Liquid Films, Fundamentals and Applications (Surfactant Science Series vol 29)* ed I B Ivanov (New York: Dekker) ch 2, pp 49–129
[12] Ash S G, Everett D H and Radke C J 1973 *J. Chem. Soc. Faraday Trans.* II **69** 1256
[13] Toshev B V and Ivanov I B 1975 *Colloid Polymer Sci.* **253** 558
[14] De Feijter J A, Rijnbout J B and Vrij A 1978 *J. Colloid Interface Sci.* **64** 258
[15] Mysels K J and Jones M N 1966 *Discuss Faraday Soc.* **42** 42
[16] Claesson P, Ederth T, Bergeron V and Rutland M W 1996 *Adv. Colloid Interface Sci.* **67** 119
[17] Bergeron V and Radke C J 1992 *Langmuir* **8** 3020
[18] Duyvis E M 1962 The equilibrium thickness of free liquid films *Thesis* Utrecht
[19] Attard P, Mitchell D J and Ninham B W 1988 *J. Chem. Phys.* **88** 4987
[20] Attard P, Mitchell D J and Ninham B W 1988 *J. Chem. Phys.* **89** 4358
[21] Derjaguin B V, Churaev N V and Muller V M 1987 *Surface Forces* ed J A Kichener (New York: Consultants Bureau)
[22] Hunter R J 1987 *Foundations of Colloid Science* vol 1 (Oxford: Clarendon)
[23] Israelachvili J N 1985 *Intermolecular and Surface Forces with Applications to Colloid and Biological Systems* (Orlando, FL: Academic)
[24] Chu B 1967 *Molecular Forces, Based on the Baker Lectures of Peter J.W. Debye* (New York: Wiley–Interscience)
[25] Usui S and Hachisu S 1984 Interaction of electrical double layers and colloid stability *Electrical Phenomena at Interfaces: Fundamentals, Measurements, and Applications (Surfactant Science Series vol 15)* ed A Kitahara and A Watanabe (New York: Dekker) pp 47–98
[26] Ohshima H 1974 *Colloid Polym. Sci.* **252** 158
[27] Ohshima H 1974 *Colloid Polym. Sci.* **252** 257
[28] Chan D, Perram J W, White L R and Healy T W 1975 *J. Chem. Soc. Faraday Trans.* **71** 1046
[29] Chan D, White L R and Healy T W 1975 *J. Chem. Soc. Faraday Trans.* **72** 2844
[30] Hamaker H C 1937 *Physica* **4** 1058
[31] Casmir H B and Polder D 1948 *Phys. Rev.* **73** 360
[32] Prausnitz J M, Lichtenthaler R N and Azevedo de E G 1986 Intermolecular forces and the theory of corresponding states *Molecular Thermodynamics of Fluid-Phase Equilibria* 2nd edn (Englewood Ciffs, NJ: Prentice-Hall) ch 4, pp 48–88
[33] Vold M J 1961 *J. Colloid Sci.* **16** 1
[34] Vincent B 1973 *J. Colloid Interface Sci.* **42** 270
[35] Dzyaloshinskii I E, Lifshitz E M and Pitaevskii L P 1959 *Advan. Phys.* **10** 165
[36] Dzyaloshinskii I E, Lifshitz E M and Pitaevskii L P 1960 van der Waals forces in liquid films *Sov. Phys.–JETP* **37** 161–70
[37] Parsegian V A 1975 Long range van der Waals forces *Physical Chemistry: Enriching Topics from Colloid and Surface Science IUPAC* ed H Olphen and K J Mysels (La Jolla, CA: Theorex) pp 27–72
[38] Parsegian V A and Ninham B W 1969 *Nature* **224** 1197
[39] Israelachvili J N and Wennerström H 1992 *J. Phys. Chem.* **96** 520
[40] Bélorgey O and Benattar J J 1991 *Phys. Rev. Lett.* **66** 313
[41] Gamba Z, Hautman J, Shelley J C and Klein M L 1992 *Langmuir* **8** 3155
[42] Bergeron V 1997 *Langmuir* **13** 3474
[43] Vrij A 1966 *Discuss. Faraday Soc.* **42** 23
[44] Vrij A and Overbeek J Th G 1968 *J. Am. Chem. Soc.* **90** 3074
[45] De Vries A 1958 *J. Recl. Trav. Chim. Pays-Bas* **77** 383
De Vries A 1958 *J. Recl. Trav. Chim. Pays-Bas* **77** 441
[46] Derjaguin B V and Prokhorov A V 1981 *J. Colloid Interface Sci.* **81** 108
[47] Kashchiev D and Exerowa D 1980 *J. Colloid Interface Sci.* **77** 501
[48] Kabalnov A and Wennertrom H 1996 *Langmuir* **12** 276
[49] Schmelzer J W P, Gutzon I and Schmelzer J 1996 *J. Colloid Interface Sci.* **178** 657
[50] Lucassen-Reynders E H 1981 *Anionic Surfactants, Lucassen-Reynders (Surfactant Science Series vol 11)* ed E H Hansen (New York: Dekker) p 173
[51] Prieve D C and Lin M N 1982 *J. Colloid Interface Sci.* **86** 17
[52] Adamczyk Z, Czarnecki J and Warszynski P 1985 *J. Colloid Interface Sci.* **106** 299
[53] Warszynski P and Czarnecki J 1989 *J. Colloid Interface Sci.* **128** 137

[54] Israelachvili J N and Pashley R 1982 *Nature* **300** 341
[55] Eriksson J C, Ljunggren S and Claesson P M 1989 *J. Chem. Soc. Faraday Trans.* II **85** 163
[56] Ruckenstein E and Churaev N 1991 *J. Colloid Interface Sci.* **147** 535
[57] Johonntt E S 1906 *Phil. Mag.* **11** 746
[58] Perrin J 1918 *Ann. Phys., Paris* **10** 160
[59] Bruil H G and Lyklema J 1971 *J. Nature Phys. Sci.* **233** 19
[60] Nikolov A D and Wasan D T 1989 *J. Colloid Interface Sci.* **133** 1
[61] Richetti P and Kékicheff P 1992 *Phys. Rev. Lett.* **68** 1951
[62] Kékicheff P and Richetti P 1992 *Pure Appl. Chem.* **64** 1603
[63] Manev E D, Sazdanova S V, Rao A A and Wasan D T 1982 *J. Dispersion Sci. Technol.* **3** 453
[64] Keuskamp J W and Lyklema J 1975 *Adsorption at Interfaces (ACS Symposium Series 8)* ed K L Mittal (Washington, DC: American Chemical Society) pp 191–8
[65] Exerowa D and Lalchev Z 1986 *Langmuir* **2** 668
[66] Wasan D T, Nikolov A D, Huang D D and Edwards D A 1988 *Surfactant-Based Mobility Control, Progress in Miscible-Flood Enhanced Oil Recovery* ed D H Smith (Washington, DC: American Chemical Society) pp 136–62
[67] Pollard M L and Radke C J 1994 *J.Chem. Phys.* **8** 6979
[68] Overbeek J Th G 1960 *J. Phys. Chem.* **64** 1181
[69] Lyklema J and Mysels K J 1965 *J. Am. Chem. Soc.* **87** 2539
[70] Nikolov A D, Kralchevsky P A, Ivanov I B and Wasan D T 1989 *J. Colloid Interface Sci.* **133** 13
[71] Perez E, Proust J E and Ter-Minassian-Saraga L 1978 *Colloid Polym. Sci.* **256** 784
[72] Perez E and Proust J E and Ter-Minassian-Saraga L 1988 Thin films from liquid crystals *Thin Liquid Films, Fundamentals and Applications (Surfactant Science Series vol 29)* ed I B Ivanov (New York: Dekker) ch 13, pp 891–25
[73] Bergeron V 1996 *Langmuir* **12** 5751
[74] Mutz M and Helfrich W 1989 *Phys. Rev. Lett.* **62** 2881
[75] Lipowsky R 1991 *Nature* **349** 475
[76] Bergeron V, Langevin D and Asnacios A 1996 *Langmuir* **12** 1550
[77] Goddard E D and Ananthapadmanablan K P 1993 *Interactions of Surfactants with Polymers and Proteins* (Boca Raton, FL: Chemical Rubber Company)
[78] Akesson T, Woodward C and Jonsson B 1989 *J. Chem. Phys.* **91** 2461
[79] Miklavic S J, Woodward C E, Jonsson B and Akesson T 1990 *Macromolecules* **23** 4149
[80] Carignano M A and Dan N 1998 *Langmuir* **14** 3475